

Dissolved organic matter characteristics and bacteriological changes during phosphorus removal using ladle furnace slag

Jin H. Noh^{1a}, Sang-Hyup Lee^{2,3b}, Jae-Woo Choi^{2b} and Sung Kyu Maeng^{*1}

¹Department of Civil and Environmental Engineering, Sejong University, 209 Neungdongro, Gwangjin-gu, Seoul 05006, Republic of Korea

²Center for Water Resource Cycle, Green City Technology Institute, Korea Institute of Science and Technology, 5, Hwarang-ro 14-gil, Seongbuk-gu, Seoul 02792, Republic of Korea

³KU-KIST Green School, Graduate School of Energy and Environment, Korea University, 145 Anam-ro, Seongbuk-gu, Seoul, 02841, Republic of Korea

(Received October 15, 2017, Revised April 30, 2018, Accepted May 1, 2018)

Abstract. A sidestream contains the filtrate or concentrate from the belt filter press, filter backwash and supernatant from sludge digesters. The sidestream flow, which heads back into the sewage treatment train, is about 1-3% less than the influent flow. However, the sidestream can increase the nutrient load since it contains high concentrations of phosphorus and nitrogen. In this study, the removal of PO₄-P with organic matter characteristics and bacteriological changes during the sidestream treatment via ladle furnace (LF) slag was investigated. The sidestream used in this study consisted of 11-14% PO₄-P and 3.2-3.6% soluble chemical oxygen demand in influent loading rates. LF slag, which had a relatively high Ca²⁺ release compared to other slags, was used to remove PO₄-P from the sidestream. The phosphate removal rates increased as the slag particle size decreased 19.1% (2.0-4.0 mm), 25.2% (1.0-2.0 mm) and 79.9% (0.5-1.0 mm). The removal rates of dissolved organic carbon, soluble chemical oxygen demand, color and aromatic organic matter (UV₂₅₄) were 17.6, 41.7, 90.2 and 77.3%, respectively. Fluorescence excitation-emission matrices and liquid chromatography-organic carbon detection demonstrated that the sidestream treatment via LF slag was effective in the removal of biopolymers. However, the removal of dissolved organic matter was not significant during the treatment. The intact bacterial biomass decreased from 1.64×10⁸ cells/mL to 1.05×10⁸ cells/mL. The use of LF slag was effective for the removal of phosphate and the removal efficiency of phosphate was greater than 80% for up to 100 bed volumes.

Keywords: hydroxyapatite; organic matter; phosphorus; slag; sidestream

1. Introduction

A sidestream produced during activated sludge treatment processes (digester supernatant, sludge thickener filtrate and belt filter press filtrate) in sewage treatment plants is generally returned to the head of the treatment plant via a primary settling tank or grit chamber. In such cases, the sidestream flow is 1-3% less than the influent flow to sewage treatment plants. However, the sidestream contains high concentrations of nutrients, such as nitrogen and phosphorus (Dosta *et al.* 2007, Hu *et al.* 2017, Ivanov *et al.* 2009, Ren *et al.* 2015). Estimates of the phosphorus load from the sidestream range between 10 and 80% of the total phosphorus in sewage treatment plants; therefore, it is important to reduce the impact of the sidestream to improve effluent phosphorus concentrations (Guo *et al.* 2010, Ivanov *et al.* 2009, Ragheb 2013, Ren *et al.* 2015, Yang *et al.* 2009). This could result in significant improvement in the

effluent quality. The conventional way is to return the sidestream to the influent, but there are more benefits in the treatment of the sidestream, which can reduce the loading on the main nutrient removal processes in sewage treatment plants or recover phosphorus for recycling. There have been recent studies concerning the treatment of the sidestream via the separate treatment (Lahav *et al.* 2013, Ivanov *et al.* 2009, Yang *et al.* 2009). Various treatment techniques can be used to remove phosphorus during sewage treatment, but the most common treatments are biological and/or physiochemical processes. Biological treatment is a cost-effective process for removing phosphorus, but it is difficult to meet the recent stringent water quality standards for total phosphorus in Korea (< 0.2 mg/L as total phosphorus). Therefore, it is necessary to apply physicochemical treatment processes, such as coagulation/precipitation, as a tertiary treatment or advanced treatments (Khulbe *et al.* 2012). The physiochemical treatment process can achieve relatively high phosphorus removal rates, but the cost is higher due to chemicals and high volumes of sludge produced. There were also attempts to save on the cost of chemicals.

Phosphate can be removed via precipitation with metal ions, including forms of aluminum phosphate, magnesium phosphate and calcium phosphate. Alum is a strong phosphate absorbent and induces precipitation immediately

*Corresponding author, Professor

E-mail: smaeng@sejong.ac.kr

^aPh.D. Student

E-mail: nowdaji@hanmail.net

^bPrincipal researcher

E-mail: yisanghyup@kist.re.kr, plead36@kist.re.kr

upon reaction, but it is strongly influenced by the characteristics and volume of organic matter in the sewage. Combined with magnesium, it can remove both nitrogen and phosphorus in the form of struvite, promoting sludge digestion and stabilization. Calcium is often recommended because it is lower in cost and easy to use. It can also be replaced by industrial by-products containing calcium such as steel slag, fly ash and biological (bivalve) shells as precipitates. There are cost effective processes via physiochemical precipitation of phosphorus, which is used in fertilizers (De-Bashan and Bashan 2004). Because these industrial by-products include large amounts of calcium oxide (CaO), high concentrations of phosphates in the sidestream can be removed via the precipitation of the calcium phosphate complex. Phosphate exists as H_2PO_4^- , HPO_4^{2-} and PO_4^{3-} at pH 9 or lower, 9-12 and 12 and higher, respectively (Ren *et al.* 2015). Of these, the most stable calcium phosphate form is hydroxyapatite ($\text{Ca}_5(\text{PO}_4)_4(\text{OH})$ or HAP). If the calcium ion (Ca^{2+}) and phosphate are under alkaline conditions ($\text{pH} > 9$), HAP generation is known to accelerate (Johansson and Gustafsson 2000; Kim *et al.* 2006). Therefore, it is important to maintain a high pH level when slag is used in the removal of phosphate.

A positively charged site in HAP is known to be advantageous in the removal of organic compounds, chromogenic materials, heavy metals and suspended particulate matter (Bahdod *et al.* 2009, Barka *et al.* 2011, Corami *et al.* 2007, Elouear *et al.* 2008). Dissolved humic substances have a negative surface charge that quickly binds to calcium phosphates generated when Ca^{2+} and PO_4^{3-} combine (Song *et al.* 2006). Previous studies have shown that when phosphate is removed using slag, a considerable amount of COD was also removed (Ragheb 2013, Yang *et al.* 2009). However, limited amount of studies have been carried out to investigate changes in organic matter characteristics during the removal of phosphate from the sidestream via the precipitation of calcium phosphate complexes.

Steel slag is the product of carbon and silicon removal and is the by-product of steel made from iron. It is categorized as basic oxygen furnace (BOF) slag and electric arc furnace (EAF) slag. EAF slag can be divided into oxidizing slag and ladle furnace (LF) slag. The CaO compositions in BOF, electric arc furnace oxidizing (EAFO) slag and LF slag from steelmaking were 44.3%, 26.2% and 51.0%, respectively. Steel slag is known to contain 0.1-20% of free CaO (Choi *et al.* 2007). CaO in slag releases Ca^{2+} and OH^- that combine with phosphate to form HAP. Therefore, it has the potential to reduce the cost of chemicals (Barca *et al.* 2012, Drizo *et al.* 2006, Kim *et al.* 2006, Kostura *et al.* 2005, Xue *et al.* 2009, Yang *et al.* 2009).

The sidestream contains a relatively high concentration of organic matter, compared to sewage and can also add an additional 20-30% to the organic matter load (Choi and Lee 1993). Also, anaerobic digester supernatant was found to have a direct effect on bulking in secondary clarifiers despite its relatively small flow rate (Erdirençelebi and Küçükhemek 2015). Thus, there is a need to reduce the impact of the sidestream in sewage treatment plants because it will increase the biomass load and operation cost. Thus,

additional treatment may be required before its return to the influent flow (Tong and Chen 2007). Previous studies have been sparsely available regarding the impact of the sidestream treatment on bacteriological changes. Moreover, when high concentrations of suspended bacterial biomass in the sidestream are returned to the primary clarifier, the biomass can discharge from a secondary clarifier and could deteriorate the effluent quality. This study aimed to evaluate the potential use of LF slag in the removal of phosphate in a fluidized bed reactor (FBR) from a real sidestream with bulk organic matter characteristics and microbial behavior.

2. Materials and methods

2.1 Sidestream

In this study, the sidestream refers to a combination of supernatants from the sludge thickening and sludge dewatering processes and was collected from a full-scale sewage treatment plant (Gyeonggi-do, Republic of Korea). A real sidestream was used to verify the behavior of LF slag in a sewage treatment plant.

2.2 Slag preparation and batch test

Industrial by-products (EAFO slag, LF slag and fly ash) collected from Dongbu Steel (Chungcheongnam-do, Korea) were used to remove the phosphate from the sidestream. A batch test was conducted to determine the performance between selected industrial by-products. Each 10 g of EAFO slag, LF slag and fly ash were dried for 24 hours at 80°C in a dry oven and used in a batch test with 1 L of deionized water. LF slag showed the highest Ca^{2+} concentration (Fig. S1) and was sorted into three grain sizes (0.5-1.0, 1.0-2.0 and 2.0-4.0 mm) to investigate the effects of grain size of LF slag on the removal of phosphate.

2.3. Laboratory-scale fluidized bed reactor

The schematic diagram of a laboratory-scale FBR is shown in Fig. 1. The sidestream was introduced at the bottom of the reactor. Ca^{2+} and OH^- , eluted from LF slag, reacted with phosphate in the sidestream. A peristaltic micro pump was used to introduce the sidestream at 30 m/h to secure the mixing in the FBR. The slag was filled to a height of 50 cm and a volume of 245 mL to prevent the loss of the slag. The effluent was stored in an effluent storage tank and a mixer was used to remove some remaining phosphate in the sidestream. Since FBR does produce excessive sludge, it is effective to treat sidestream in order to reduce phosphorus that flows back into a primary clarifier.

2.4 Analysis Method

The pH and conductivity were measured by HQ40d-PHC301 (Hach, U.S.A.) and Cond 6641 SET1 (WTW, Germany), respectively. Samples filtered with a 0.45- μm filter (Whatman, U.S.A.) were analyzed according to the

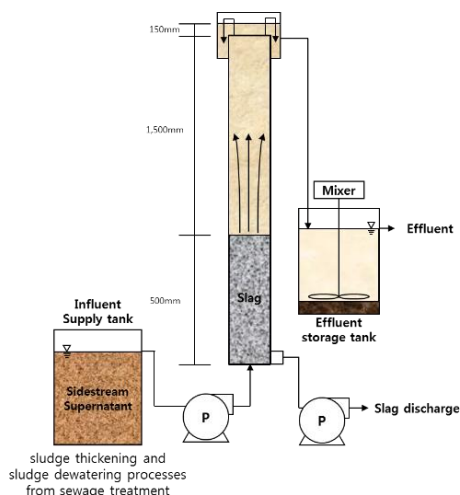


Fig. 1 Schematic diagram of Lab-scale fluidized bed reactor

standard methods for phosphate and soluble chemical oxygen demand (COD) (Federation, W. E. and American Public Health Association 2005). Calcium (Ca^{2+}), magnesium (Mg^{2+}) and aluminum (Al^{3+}) concentrations were measured by an inductively coupled plasma-optical emission spectrometer (ICP-OES, ICAP-6300, Thermo Scientific, U.S.A.). To analyze the dissolved organic carbon (DOC), a total organic carbon (TOC) analyzer (TOC-V CPN, Shimadzu, Japan) was used and a UV/Vis spectrophotometer (DR-5000, Hach, U.S.A.) was used to measure the ultraviolet absorbance at 254 nm (UV_{254}). DOC concentration was diluted to less than 10 ppm using deionized water (dilution factor of 3). Color was measured using the platinum cobalt standard method. A liquid chromatography-organic carbon detector (LC-OCD, DOC-LABOR, Germany) was used to determine organic matter fractions into biopolymers, humic substances, building blocks, low molecular weight (LMW) neutrals and LMW organic acids (Huber *et al.* 2011). Fluorescence intensity according to four wavelength regions of the fluorescence excitation (ex)-emission (em) matrices (EEM) was measured using a quartz cuvette (Hellma, U.S.A.) with a fluorescence spectrophotometer (RF5301-pc, Shimadzu, Japan). There are four regions related to protein-like and humic-like substances and they are protein-like peak T1 (ex/em = 220-240 / 320-350 nm), tryptophan protein-like peak T2 (ex/em = 270-280 / 320-350 nm), fulvic-like peak A (ex/em = 250-260 / 380-480 nm) and humic-like peak C (ex/em = 330-350 / 420-480 nm) (Westerhoff and Pinney 2000). X-ray diffraction (XRD) analysis (ATX-G, Rigaku, Japan) and X-ray fluorescence (XRF) (RIX2100, Rigaku, Japan) were used to determine the surface characteristics and EDS (Energy Dispersive x-ray Spectroscopy; S-4700, Hitachi, Japan) was used to analyze the chemical composition.

To determine the intact bacterial biomass, sonication was performed on 100 mL of each sample using an ultrasonifer (Cole-Parmer 8890, Vernon Hills, IL) at 100 kJ/L (20 kHz, 130 Watt, 77 s) (Kostura *et al.* 2005). After dyeing with a reagent that is a mixture of SYBR Green I and propidium iodide (PI), intact cells and damaged cells

Table 1 Characteristics of the sidestream collected from the S sewage treatment plant (Gyeonggi-do, South Korea) during the experiments (n=7)

Parameter	
pH (-)	6.92±0.4
Conductivity (ms/cm)	1.15±0.3
DOC (mg/L)	259.0±61.3
UV_{254} (cm^{-1})	1.32±0.3
Color (PtCO)	941.6±95.2
T-P (mg/L as P)	95.7±25.7
$\text{PO}_4\text{-P}$ (mg/L as P)	54.5±11.7
Total N (mg/L as N)	252.6±46.9
Soluble N (mg/L as N)	93.4±8.6
Total COD (mg/L)	1296.6±145.3
Soluble COD (mg/L)	758.8±82.4
Ca^{2+} (mg/L)	25.1±4.8
Mg^{2+} (mg/L)	19.3±2.7

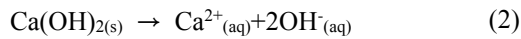
were counted using a flow cytometer equipped with a 20-mW blue diode pumped solid-state laser at 488 nm (CyFlow Cube6, Partec GmbH, Germany). SYBR Green I is able to penetrate the membrane of intact cells to combine with DNA and RNA. However, PI cannot penetrate an intact cell membrane that cannot be dyed, making them easy to be differentiated from damaged cells. A more detailed explanation of the apparatus and measurement of bacteria cell via flow cytometry have been reported elsewhere (Berney *et al.* 2008) and plots were prepared using FCS4 Express Cytometry software (De Novo Software).

3. Results and discussion

3.1 Influent characteristics and laboratory-scale fluidized bed reactor experiment

Characteristics of the sidestream over a set period of time are shown in Table 1. The average concentration of phosphate in the sidestream was relatively high (54.5 mg/L as P) and found to be significant when comprising 11-14% of the sidestream, which flows back into sewage treatment train. The average concentrations of total COD and soluble COD were 1296.6 and 758.8 mg/L, respectively. In the preliminary test, LF slag showed the highest concentration of Ca^{2+} among selected industrial by-products and the removal of phosphate varied by different steel slags (LF slag (14.9 ± 0.9 g/kg) > fly ash (3.1 ± 0.1 g/kg) > EAFO slag (1.6 ± 0.1 g/kg)) (Fig. S1). LF slag was also reported to be most effective on the removal of phosphate (Lee and Lee 2007). As shown in Fig. 2, free CaO on the slag surface was initially eluted in excess (510.6 mg/L of Ca^{2+}) at a pH of 12.7. There was a sudden increase in pH and electrical conductivity upon making contact with deionized water. The increase of electrical conductivity clearly showed that the concentration of ions from the slag gradually decreased

with respect to bed volumes (BVs) and well corresponded with result of calcium concentration. As shown in the chemical equations below, the Ca^{2+} and OH^- ion concentrations increased because of the $\text{Ca}(\text{OH})_{2(s)}$, which was formed via reaction (Eq. (1)) and was quickly dissolved (Eq. (2)). These results are also similar to results from other studies that performed batch experiments using slag (Kim *et al.* 2010). The removal of phosphate in the sidestream was observed via reaction (Eq. (3)).



As BV increased, the dissolution of LF slag decreased, which resulted in a decrease in Ca^{2+} and OH^- . Ca^{2+} and pH were 124 mg/L and 11.9, respectively, at 250 BV (Fig. 2). The concentration of Ca^{2+} was 167.8 mg/L at 100 BV and the sidestream had a phosphorus concentration of 45.1 ± 15.6 mg/L. HAP crystallization is most effective at a Ca/P ratio = 2 and a pH of at least 9 (Johansson and Gustafsson 2000, Kim *et al.* 2006). When considering the maximum phosphate concentration of 78.5 mg/L in the sidestream, 100 BV was most appropriate for the removal of phosphate in the FBR. In this study, the removal of phosphate from the sidestream was determined at 100 BV.

3.2 Removal of phosphate in the sidestream according to slag size

Concentrations of Ca^{2+} in the FBR using LF slag varied with the different grain sizes of 0.5-1.0 mm, 1.0-2.0 mm and 2.0-4.0 mm and were decreased as the LF slag size increased (643.9 mg/L for 0.5-1.0 mm, 340.5 mg/L for 1.0-2.0 mm and 196.6 mg/L for 2.0-4.0 mm) (Fig. S2). Ca^{2+} was confirmed to be eluted in excess during the beginning of the experiment (BV < 25). For up to 100 BV, the average removal rates of phosphate were 79.9%, 25.2% and 19.1% for LF slag sizes of 0.5-1.0 mm, 1.0-2.0 mm and 2.0-4.0 mm, respectively (Fig. 3). The specific surface area

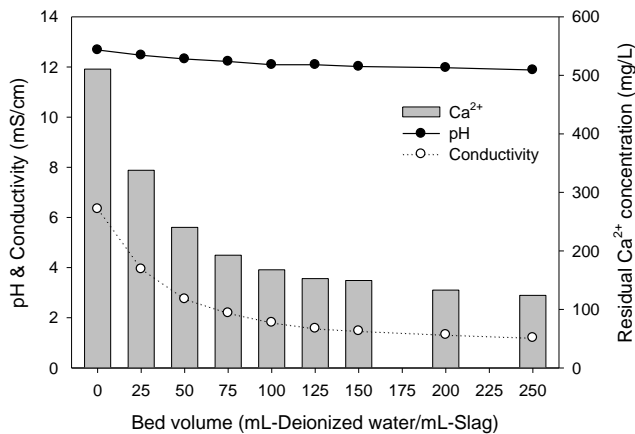


Fig. 2 Changes in pH, conductivity and residual Ca^{2+} concentration in deionized water with ladle furnace slag (0.5-1.0 mm) for up to 250 BV

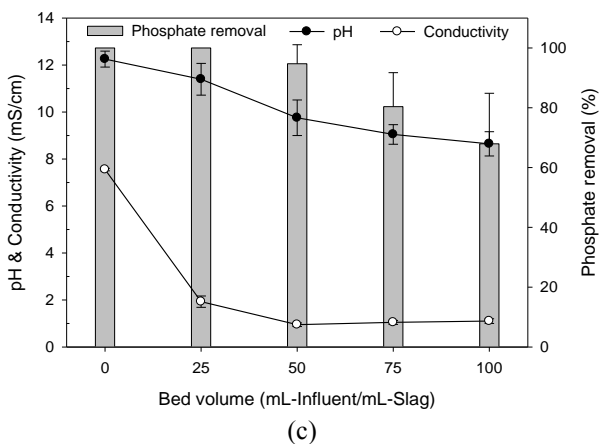
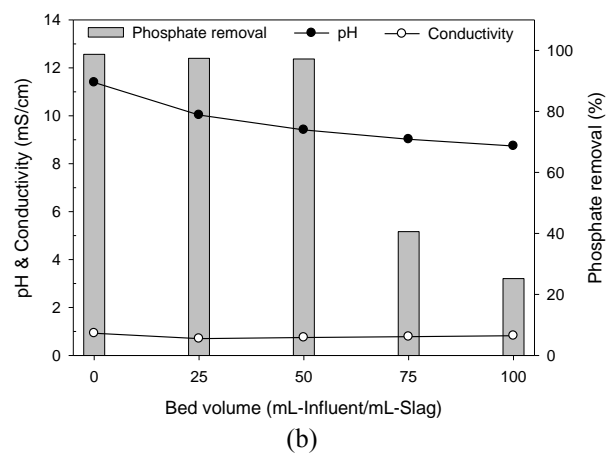
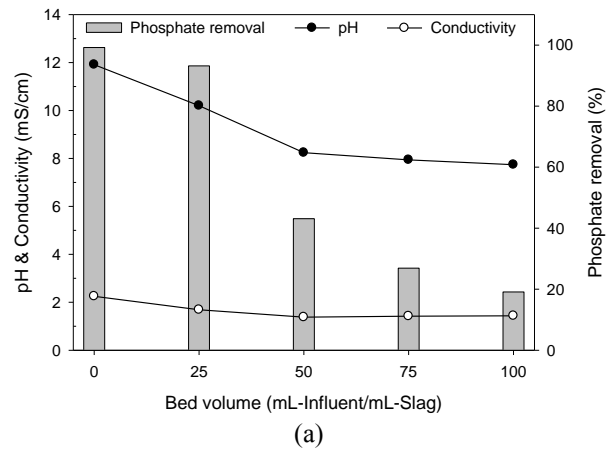


Fig. 3 Removal of phosphate with pH and conductivity using different grain sizes of ladle furnace slag; (a) 2.0-4.0 mm, (b) 1.0-2.0 mm and (c) 0.5-1.0 mm

of the slag increases as grain size decreases. As the particle size of the slag becomes smaller, more CaO is available for HAP formation, which leads to higher Ca^{2+} and OH^- concentrations in the FBR. Therefore, the removal rate of phosphate was enhanced as the grain size of LF slag decreased and similar results were also observed in previous studies (Lee *et al.* 2010, Lee and Lee 2007). It is also known that the precipitation of calcium phosphate was

effective at pH 9 or higher (Johansson and Gustafsson 2000, Kim *et al.* 2006). In our study, the phosphate removal rates were effective up to 100 BV with the particle size of slag between 0.5-1.0 mm at pH > 9.0. The removal of phosphate was accelerated under alkaline conditions (pH > 9) and the slag should change for every 100 BV to maintain pH > 9 in the FBR.

3.3 Surface characteristics of LF slag

After conducting the laboratory-scale FBR up to 100 BV, the slag was extracted from the reactor for an investigation of its surface characteristics. An analysis was performed after the slag was dried at 80°C for 24 h in a dry oven. From the EDS analysis results (Fig. S3), the raw slag components consist of Ca (25.7%), C (4.8%) and O (56.8%). After the laboratory-scale FBR was run for up to 100 BV, the content ratio of Ca, C and O were calculated at 21.1%, 7.5% and 52.7%, respectively. The Ca and O content had slightly decreased and similar results were also confirmed by XRF analysis. The CaO content before was 60.6%, but it slightly decreased by 3% (to 57.6%) after 100 BV was reached (Table 2). Also, peaks in the 2 θ (degree) value in the XRD analysis for Ca(OH)₂ and Ca₃Al₂(OH)₁₂ were at 34.14° and 39.31°, respectively. Both of these peaks decreased after 100 BV was reached (Fig. S4). Based on the surface characteristics via EDS and XRD, the chemical composition of LF did not change significantly.

3.4 Changes in DOC, SCOD, color and bulk organic matter characteristics

To assess the fate of bulk organic matter in the sidestream, DOC, SCOD and UV₂₅₄ were performed at BV of 0, 25, 50, 75 and 100. As shown in Fig. 4, the removal rates for soluble COD and color at BV < 50 were significant. Removal rates of DOC and soluble COD were 11.5% and 13.2%, respectively, at 100 BV. Moreover, the removal of color was reduced from 91% to 49% at BV < 25, but it decreased to 36.9% at 100 BV. Removal of bulk organic matter is expected to be due to coagulation by multi-valent cation ions (Ca²⁺, Mg²⁺ and Al³⁺) eluted from the slag and precipitation. It is also considered to be partially removed by adhesion of the HAP crystal produced. Alkali decomposition of bulk organic matter as a result of high pH decreased the average molecular weight and UV/vis absorbance when organic matter was decomposed by hydroxyl group (Brinkmann *et al.* 2003). As BV increased, the free CaO eluted from the slag decreased; thus, the removal of bulk organic matter by coagulation, adhesion and alkaline hydrolysis was not significant.

Fluorescence characteristics in dissolved organic matter were measured using EEM spectra. The order of fluorescence intensity for peak regions in the sidestream was T1 > T2 > A > C and the protein-like peaks (T1 and T2) were relatively high due to the destruction of cell membranes during the thickening and dehydration processes (Lee and Park 2008). The bulk organic matter removal can be confirmed through the reduction in intensity in the peak regions of T1, T2, A and C. As shown in Fig. 5,

Table 2 Chemical composition of ladle furnace slag before and after 100 BV using XRF analysis

Component	CaO	Al ₂ O ₃	MgO	SO ₃	Fe ₂ O ₃	SiO ₂	Cr ₂ O ₃	K ₂ O	etc
Mass Before (%)	60.6	26.6	4.22	3.15	3.30	1.62	0.0682	0.0209	0.4209
Mass After (%)	57.6	24.9	4.10	3.12	2.69	1.70	0.0629	0.0187	5.8084

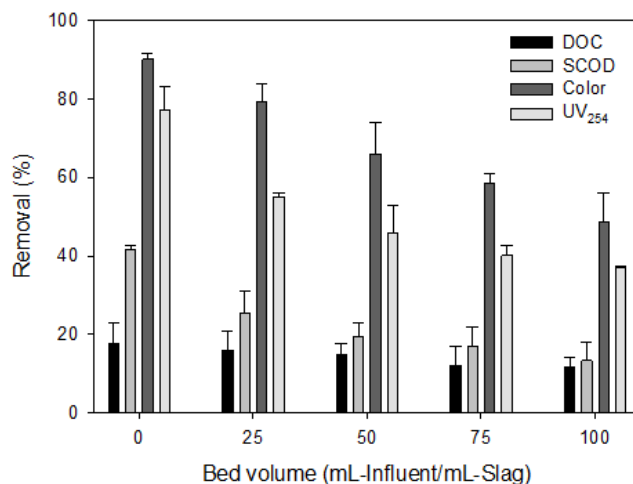


Fig. 4 Changes in DOC, SCOD, color and UV₂₅₄ with ladle furnace slag (0.5-1.0 mm) for up to 100 BV

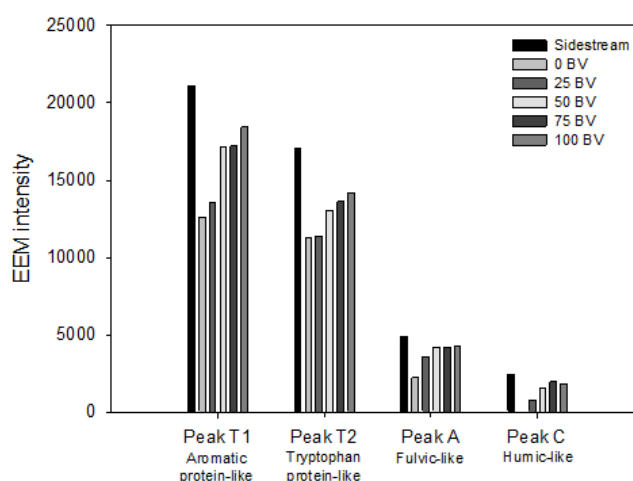


Fig. 5 Fluorescence intensities of peak regions T1, T2, A and C with ladle furnace slag at 100 BV

the fluorescent intensity decreased significantly in all peak regions at BV < 50 and the percent reduction in peak regions for C, A, T1 and T2 were 99%, 54.9%, 40.3% and 33.9%, respectively.

In terms of reduction rates, peak regions C and A were significantly decreased and T1 and T2 in the sidestream were found to be significantly high. Humic-like substances (e.g., humic acid and fulvic acid) and protein-like substances form insoluble complexes with multi-valent cation ions, such as calcium and precipitate. With an auxiliary removal mechanism, HAP crystals in the form of calcium phosphate are known to have an amphoteric charge-both a positively charged Ca site and a negatively charged PO₄ site. Acid molecules can be adsorbed on PO₄ sites and basic molecules can be adsorbed to Ca sites

(Martinson and Wagenaar 1974). As BV increased, the fluorescent intensity in peak regions increased and the reduction rates at 100 BV for C, T2, A and T1 were found to be 24.9%, 17.1%, 13.5% and 12.7%, respectively. At low BV, the fluorescent intensities at peak regions decreased significantly due to dissolved organic matter (e.g., protein-like substances), which are coagulated by multi-valent and are adsorbed on the crystals. However, as BV increased, the reduction of fluorescence intensities at peak regions decreased as the removal of phosphate decreased.

The effect of sidestream treatment via LF slag on the fate of bulk organic matter characteristics in the sewage treatment plant process was investigated. The fluorescent properties for each treatment step in a full-scale sewage treatment plant are shown in Fig. 6 and the protein-like peak was generally high. We determined the influence of the sidestream before and after the sidestream treatment via LF slag and the order was found to be peak T2 (7.9%), T1 (6.8%), A, (1.87%) and C (0.13%) before treatment. After the treatment, the peak regions did not significantly change: T2 (7.1%), T1 (6.5%), A (1.7%), peak C (0.09%). Comparison of the influence of before and after sidestream treatment showed that the effect was less than 1% in peak regions (peak T2 0.8%, peak T1 0.3%, peak A 0.17%, peak C 0.04%).

LC-OCD analysis of each process in the sewage treatment plant before and after treatment is also shown in Fig. 7 and the concentration of all substances except LMW acids was much higher in the sidestream. There was a relatively large decrease in biopolymers (29.5%) and building blocks (34.6%), but the decrease was not so significant for humic substances (3.7%) and LMW neutrals (1.2%). Biopolymers are composed of organic colloids and high molecular weight protein substances. Thus, the removal rate through adsorption and precipitation was high. Based on the above results, the organic matter characteristics were slightly changed during the sidestream treatment.

3.5 Intact bacterial biomass

As shown in Fig. 8, the bacteriological change in the sidestream was determined using flow cytometry. There were 1.69×10^8 cells/mL (intact cells) in the sidestream and the reduction of intact cells was due to a high pH of 12.5 via the destruction of cell membrane at the initial BVs. The reduction of intact cells was due to a high pH of 12.5 via the destruction of the cell membrane at low BV. It is known that when the pH is above 11, the cell membrane is damaged, which leads to the release of intracellular substances such as deoxyribonucleic acid (DNA) (Becerra *et al.* 2010). Bacteria are known to become inactive under alkaline conditions (pH 8-12) (Nilsson *et al.* 2013). In previous studies, the bacterial mortality rate was 98.6%, 99.4% and 99.4% for aerobes, fecal coliforms and fecal streptococci, respectively, after 1 h at 20°C and pH 11 (Dague *et al.* 1980).

In Fig. 3(c), the removal rate of phosphate at 25 BV was > 99%, which was the same as at 1 BV. However, the reduction rate of intact cells decreased to 85.3%. The reduction rate was relatively high when pH was 12 or

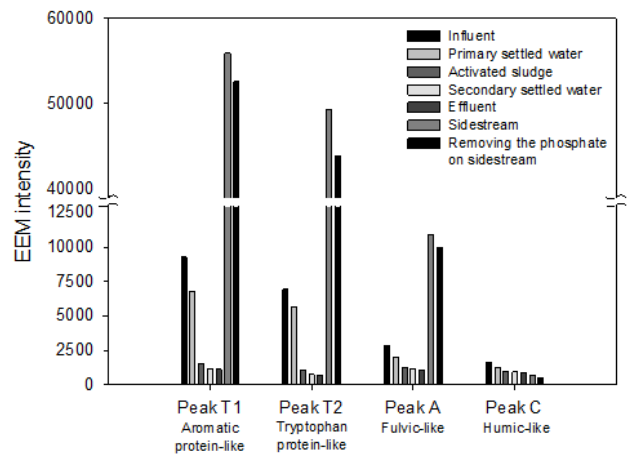


Fig. 6 Fluorescence intensities of peak regions T1, T2, A and C in sewage treatment steps

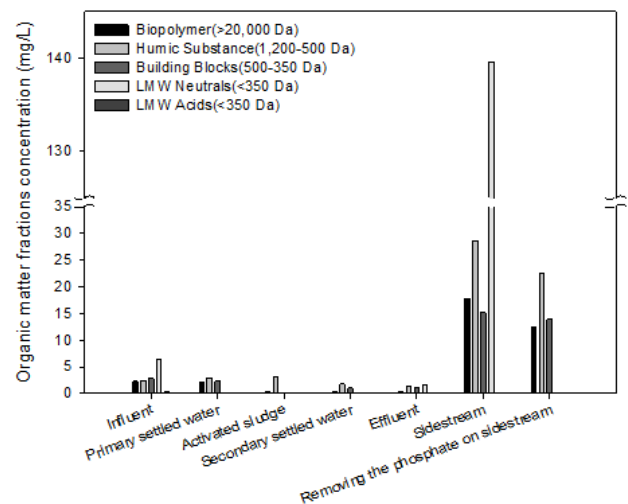


Fig. 7 Changes in organic matter fractions determined by LC-OCD (biopolymers, humics, building blocks, low molecular weight neutrals and acids in sewage treatment steps)

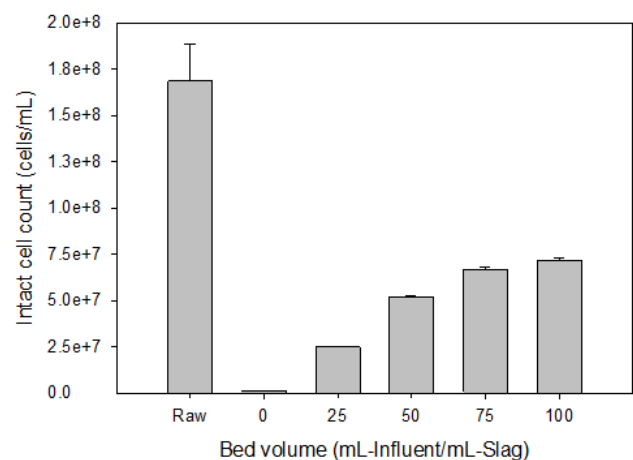


Fig. 8 The reduction of intact cells during the sidestream treatment using ladle furnace slag for up to 100 BV

higher. Also, intact cells during the sidestream treatment are gradually increased and the reduction rates of intact cells

decreased by 57.5% at 100 BV. In order to determine the intact cells that were removed through precipitation, Ca^{2+} was spiked at $\text{Ca}/\text{P} = 2$ based on the dissolved phosphorus in the sidestream. Then, 0.1 M NaOH was used to adjust the pH to 9.5 and to investigate the effect of pH on the reduction of intact cells with phosphate removal. Precipitates were sonicated and an intact cell analysis was performed. The results showed that the phosphate removal rate was > 99% and there were 5.1×10^9 cells/mL (intact cells) that had been extracted from the precipitates, which was 9.1 times higher than that before treatment (5.6×10^8 cells/mL). At pH 9.5 without adding Ca^{2+} , the phosphate removal rate was 62.1% and 3.0×10^8 cells/mL of intact cells were extracted from the precipitates, which is 5.4 times more than that of the sidestream raw water (Fig. S5). Considering the number of intact cells that were extracted from the precipitates compared to that of the sidestream, it is clearly demonstrated that there was further removal due to precipitation apart from the removal due to high pH.

Furthermore, the bacterial biomass in the sewage treatment plant processes was investigated to help in understanding the intact bacterial biomass in a full-scale sewage treatment plant with the sidestream treatment via LF slag (Fig. S6). The number of intact cells in the overall process were shown to be in order: activated sludge (1.29×10^9 cells/mL), primary settled water (1.67×10^8 cells/mL), influent (1.64×10^8 cells/mL), secondary settled water (1.24×10^7 cells/mL) and effluent (7.83×10^6 cells/mL). This was similar to previous studies (Foladori *et al.* 2010, Ma *et al.* 2013). Intact cells before and after the sidestream treatment were 5.61×10^8 and 1.05×10^8 cells/mL, respectively (81.4% removal rate). The concentration of intact cells in the sidestream was less than in the influent. Therefore, there would be almost no effect on the intact bacterial biomass if the sidestream returns to the sewage treatment plant after LF slag treatment.

4. Conclusions

In this study, LF slag was used to remove high concentrations of phosphate from a sidestream in order to reduce the nutrient load in sewage treatment plants. In the laboratory-scale FBR test, the maximum phosphate concentration observed in the sidestream was 78.5 mg/L and the removal of phosphate was greater than 80% for up to 100 BV. Considering the removal rates of phosphate according to slag particle size (0.5-1.0, 1.0-2.0 and 2.0-4.0 mm), 0.5-1.0 mm of slag removed 79.9% of phosphate with 643.9 mg/L of Ca^{2+} . The removal rates of DOC, soluble COD and UV_{254} were 17.6%, 41.7% and 77.3%, respectively. Although relatively high removal rates of phosphate were observed at low BV, the removal rate gradually decreased as BV increased. The concentration of Ca^{2+} and pH also decreased with BV. The fluorescence properties of organic matter were removed by 24.9%, 17.1%, 13.5% and 12.7% according to the intensities of the peak regions of C, T2, A and T1, respectively, at 100 BV. LC-OCD results showed that the reduction rates of biopolymers, building blocks, humic substances and LMW neutrals were 29.5%, 34.6%, 3.7% and 1.2%, respectively.

There was a 99.2% reduction of intact cell observed in the sidestream at 25 BV. Upon comparison at higher BV, the degree of the intact cell reduction was relatively large at pH 9 or higher. However, precipitation is also important in the removal of biomass during sidestream treatment using LF slag.

Acknowledgments

This work was supported by KIST Institutional Program (Project No. 2E24280) and was partially supported by Korea Ministry of Environment(MOE) through Waste to Energy Recycling Human Resource development Project.

References

- Bahdod, A., El Asri, S., Saoiabi, A., Coradin, T. and Laghzizil, A. (2009), "Adsorption of phenol from an aqueous solution by selected apatite adsorbents: Kinetic process and impact of the surface properties", *Water Res.*, **43**(2), 313-318.
- Barca, C., Gérente, C., Meyer, D., Chazarenc, F. and Andrès, Y. (2012), "Phosphate removal from synthetic and real wastewater using steel slags produced in Europe", *Water Res.*, **46**(7), 2376-2384.
- Barka, N., Qourzal, S., Assabbane, A., Nounah, A. and Ait-Ichou, Y. (2011), "Removal of Reactive Yellow 84 from aqueous solutions by adsorption onto hydroxyapatite", *J. Saudi. Chem. Soc.*, **15**(3), 263-267.
- Becerra, F.Y.G., Acosta, E.J. and Allen, D.G. (2010), "Alkaline extraction of wastewater activated sludge biosolids", *Bioresour. Technol.*, **101**(18), 6972-6980.
- Berney, M., Vital, M., Hülshoff, I., Weilenmann, H.U., Egli, T. and Hammes, F. (2008), "Rapid, cultivation-independent assessment of microbial viability in drinking water", *Water Res.*, **42**(14), 4010-4018.
- Brinkmann, T., Abbt-Braun, G. and Frimmel, F.H. (2003), "Alkaline Degradation of Dissolved Organic Matter", *Acta Hydrochim. Hydrobiol.*, **31**(3), 213-224.
- Choi, E.S. and Lee, H.S. (1993), "The sidestream from WWTP; Its characteristics and effects on the main process", *J. Civil. Eng.*, **13**(1), 233-241.
- Choi, S.W., Kim, V., Chang, W.S. and Kim, E.Y. (2007), "The present situation of production and utilization of steel slag in Korea and other countries", *J. Korea Concrete Inst.*, **19**(6), 28-33.
- Corami, A., Mignardi, S. and Ferrini, V. (2007), "Copper and zinc decontamination from single- and binary-metal solutions using hydroxyapatite", *J. Hazard. Mater.*, **146**(1), 164-170.
- Dague, R.R., Veenstra, J.N., McKim, T.W., Ashenmacher, T.G. and Lannon, J.M. (1980), "High pH Treatment of Combined Water Softening and Wastewater Sludges", *J. Water Pollut. Control Federation*, **52**(8), 2204-2219.
- De-Bashan, L.E. and Bashan, Y. (2004), "Recent advances in removing phosphorus from wastewater and its future use as fertilizer (1997-2003)", *Water Res.*, **38**(19), 4222-4246.
- Dosta, J., Galí, A., El-Hadj, T.B., Macé, S. and Mata-Alvarez, J. (2007), "Operation and model description of a sequencing batch reactor treating reject water for biological nitrogen removal via nitrite", *Bioresour. Technol.*, **98**(11), 2065-2075.
- Drizo, A., Forget, C., Chapuis, R.P. and Comeau, Y. (2006), "Phosphorus removal by electric arc furnace steel slag and serpentinite", *Water Res.*, **40**(8), 1547-1554.
- Elouear, Z., Bouzid, J., Boujelben, N., Feki, M., Jamoussi, F. and

- Montiel, A. (2008), "Heavy metal removal from aqueous solutions by activated phosphate rock", *J. Hazard. Mater.*, **156**(1), 412-420.
- Erdirençelebi, D. and Küçükhemek, M. (2015), "Diagnosis of the anaerobic reject water effects on WWTP operational characteristics as a precursor of bulking and foaming", *Water Sci. Technol.*, **71**(4), 572-579.
- Federation, W.E. and American Public Health Association (2005), *Standard Methods for the Examination of Water and Wastewater*, American Public Health Association (APHA), U.S.A..
- Foladori, P., Bruni, L., Tamburini, S. and Ziglio, G. (2010), "Direct quantification of bacterial biomass in influent, effluent and activated sludge of wastewater treatment plants by using flow cytometry", *Water Res.*, **44**(13), 3807-3818.
- Guo, C.H., Stabnikov, V. and Ivanov, V. (2010), "The removal of nitrogen and phosphorus from reject water of municipal wastewater treatment plant using ferric and nitrate bioreductions", *Bioresour. Technol.*, **101**(11), 3992-3999.
- Hu, D., Zhou, Z., Niu, T., Wei, H., Dou, W., Jiang, L.M. and Lv, Y. (2017), "Co-treatment of reject water from sludge dewatering and supernatant from sludge lime stabilization process for nutrient removal: A cost-effective approach", *Sep. Purif. Technol.*, **172**, 357-365.
- Huber, S.A., Balz, A., Abert, M. and Pronk, W. (2011), "Characterisation of aquatic humic and non-humic matter with size-exclusion chromatography-organic carbon detection-organic nitrogen detection (LC-OCD-OND)", *Water Res.*, **45**(2), 879-885.
- Ivanov, V., Kuang, S., Stabnikov, V. and Guo, C. (2009), "The removal of phosphorus from reject water in a municipal wastewater treatment plant using iron ore", *J. Chem. Technol. Biotechnol.*, **84**(1), 78-82.
- Johansson, L. and Gustafsson, J.P. (2000), "Phosphate removal using blast furnace slags and opoka-mechanisms", *Water Res.*, **34**(1), 259-265.
- Khulbe K.C., Feng C.Y., Matsuura T. and Ismail A.F. (2012), "Progresses in membrane and advanced oxidation processes for water treatment", *Membr. Water Treat.*, **3**(3), 181-200.
- Kim, E.H., Yim, S.B., Jung, H.C. and Lee, E.J. (2006), "Hydroxyapatite crystallization from a highly concentrated phosphate solution using powdered converter slag as a seed material", *J. Hazard. Mater.*, **136**(3), 690-697.
- Kim, J.W., Seo, J.B., Kang, M.G., Kim, I.D. and Oh, K.J. (2010), "A study on phosphate removal characteristic of EAF slag for submarine cover material", *Clean Technol.*, **16**(4), 258-264.
- Kim, T.H. and Park, K.B. (2000), "Swine Wastewater Treatment by using Steel-making Slag", *Clean Technol.*, **6**(2), 85-92.
- Kostura, B., Kulveitova, H. and Leško, J. (2005), "Blast furnace slags as sorbents of phosphate from water solutions", *Water Res.*, **39**(9), 1795-1802.
- Lahav, O., Telzhensky, M., Zewuhn, A., Gendel, Y., Gerth, J., Calmano, W. and Birnhack, L. (2013), "Struvite recovery from municipal-wastewater sludge centrifuge supernatant using seawater NF concentrate as a cheap Mg (II) source", *Sep. Purif. Technol.*, **108**, 103-110.
- Lee, C.W., Jeon, H.P. and Kwon, H.B. (2010), "Physical properties of pyrolyzed oyster shell consisting of porous CaO/CaCO₃ and phosphorus removal efficiency", *J. Kor. Ceram. Soc.*, **47**(6), 524-528.
- Lee, C.Y. and Park, S.Y. (2008) "Improvement of solubilization and anaerobic biodegradability for sewage sludge using ultrasonic pre-treatment", *J. Org. Resour. Recycl. Assoc.*, **16**(3), 83-90.
- Lee, S.H. and Lee, I.G. (2007), "Phosphate removal in the wastewater by the different size of granular converter slag", *J. Kor. Acad-Ind. Coop. Soc.*, **8**(1), 136-142.
- Ma, L., Mao, G., Liu, J., Yu, H., Gao, G. and Wang, Y. (2013), "Rapid quantification of bacteria and viruses in influent, settled water, activated sludge and effluent from a wastewater treatment plant using flow cytometry", *Water Sci. Technol.*, **68**(8), 1763-1769.
- Martinson, H. and Wagenaar, E. (1974), "Hydroxylapatite-catalyzed degradation of ribonucleic acid", *Biochemistry*, **13**(8), 1641-1645.
- Nilsson, C., Renman, G., Westholm, L.J., Renman, A. and Drizo, A. (2013), "Effect of organic load on phosphorus and bacteria removal from wastewater using alkaline filter materials", *Water Res.*, **47**(16), 6289-6297.
- Ping, Q., Li, Y., Wu, X., Yang, L. and Wang, L. (2016), "Characterization of morphology and component of struvite pellets crystallized from sludge dewatering liquor: Effects of total suspended solid and phosphate concentrations", *J. Hazard. Mater.*, **310**, 261-269.
- Ragheb, S.M. (2013), "Phosphate removal from aqueous solution using slag and fly ash", *HBRC. J.*, **9**(3), 270-275.
- Ren, W.C., Zhou, Z., Jiang, L.M., Hu, D.L., Qiu, Z., Wei, H.J. and Wang, L.C. (2015), "A cost-effective method for the treatment of reject water from sludge dewatering process using supernatant from sludge lime stabilization", *Sep. Purif. Technol.*, **142**, 123-128.
- Song, Y.H., Hoffmann, E. and Weidler, P.G. (2006), "Effect of humic substances on the precipitation of calcium phosphate" *J. Environ. Sci.*, **18**(5), 852-857.
- Tong, J. and Chen, Y. (2007), "Enhanced biological phosphorus removal driven by short-chain fatty acids produced from waste activated sludge alkaline fermentation", *Environ. Sci. Technol.*, **41**(20), 7126-7130.
- Westerhoff, P. and Pinney, M. (2000), "Dissolved organic carbon transformations during laboratory-scale groundwater recharge using lagoon-treated wastewater", *Waste Manage.*, **20**(1), 75-83.
- Xue, Y., Hou, H. and Zhu, S. (2009), "Characteristics and mechanisms of phosphate adsorption onto basic oxygen furnace slag", *J. Hazard. Mater.*, **162**(2), 973-980.
- Yang, J., Wang, S., Lu, Z. and Lou, S. (2009), "Converter slag-coal cinder columns for the removal of phosphorous and other pollutants", *J. Hazard. Mater.*, **168**(1), 331-337.
- Yang, Y., Zhao, Y.Q., Babatunde, A.O. and Kearney, P. (2009), "Two strategies for phosphorus removal from reject water of municipal wastewater treatment plant using alum sludge", *Water Sci. Technol.*, **60**(12), 3181-3188.

CC